



Published in final edited form as:

Cell Metab. 2014 September 2; 20(3): 512–525. doi:10.1016/j.cmet.2014.06.010.

The PPAR α - FGF21 hormone axis contributes to metabolic regulation by the hepatic JNK signaling pathway

Santiago Vernia¹, Julie Cavanagh-Kyros^{1,2}, Luisa Garcia-Haro^{1,8}, Guadalupe Sabio³, Tamera Barrett^{1,2}, Dae Young Jung¹, Jason K. Kim^{1,4}, Jia Xu^{5,9}, Hennady P. Shulha⁵, Manuel Garber^{1,6}, Guangping Gao⁷, and Roger J. Davis^{1,2,*}

¹Program in Molecular Medicine, University of Massachusetts Medical School, Worcester, Massachusetts 01605, USA

²Howard Hughes Medical Institute, Worcester, Massachusetts 01605, USA

³Department of Vascular Biology and Inflammation, Fundación Centro Nacional de Investigaciones Cardiovasculares Carlos III, 28029 Madrid, Spain

⁴Department of Medicine, Division of Endocrinology, Metabolism and Diabetes, University of Massachusetts Medical School, Worcester, Massachusetts 01605, USA

⁵Bioinformatics Core, University of Massachusetts Medical School, Worcester, Massachusetts 01605, USA

⁶Program in Bioinformatics, University of Massachusetts Medical School, Worcester, Massachusetts 01605, USA

⁷Gene Therapy Center, University of Massachusetts Medical School, Worcester, Massachusetts 01605, USA

Abstract

The cJun NH₂-terminal kinase (JNK) stress signaling pathway is implicated in the metabolic response to the consumption of a high fat diet, including the development of obesity and insulin

© 2014 Elsevier Inc. All rights reserved.

*To whom correspondence should be addressed: Roger.Davis@Umassmed.edu.

⁸Present address: Department of Cancer Biology, Dana Farber Cancer Institute, Boston, MA 02215, USA.

⁹Present address: KEW Group, 790 Memorial Drive, Suite 101, Cambridge, MA 02139, USA.

ACCESSION NUMBERS

Gene expression data were deposited (accession number GSE55190) in the Gene Expression Omnibus: <http://www.ncbi.nlm.nih.gov/geo>

SUPPLEMENTAL INFORMATION

Supplemental Information includes Supplemental Experimental Procedures and 7 figures and can be found with the article online at <http://>

AUTHOR CONTRIBUTIONS

S.V., G.S., & R.J.D. designed the study; experimental analysis was performed by S.V., J.C-K., L.G-H., & T.B.; metabolic cage & clamp studies were performed by D.Y.J. & J.K.K.; viral vectors were amplified by G.G.; bioinformatic analysis was performed by J.X., H.P.S. & M.G.; and S.V. & R.J.D. wrote the manuscript.

Publisher's Disclaimer: This is a PDF file of an unedited manuscript that has been accepted for publication. As a service to our customers we are providing this early version of the manuscript. The manuscript will undergo copyediting, typesetting, and review of the resulting proof before it is published in its final citable form. Please note that during the production process errors may be discovered which could affect the content, and all legal disclaimers that apply to the journal pertain.

resistance. These metabolic adaptations involve altered liver function. Here we demonstrate that hepatic JNK potently represses the nuclear hormone receptor peroxisome proliferator-activated receptor α (PPAR α). JNK therefore causes decreased expression of PPAR α target genes that increase fatty acid oxidation / ketogenesis and promote the development of insulin resistance. We show that the PPAR α target gene *fibroblast growth factor 21* (*Fgf21*) plays a key role in this response because disruption of the hepatic PPAR α - FGF21 hormone axis suppresses the metabolic effects of JNK-deficiency. This analysis identifies the hepatokine FGF21 as a critical mediator of JNK signaling in the liver.

Introduction

The cJun NH₂-terminal kinase (JNK) signaling pathway plays an important role in the development of obesity and insulin resistance (Sabio and Davis, 2010). Indeed, JNK1-deficiency in mice prevents the obesity and insulin resistance caused by hyperphagia or the consumption of a high fat diet (HFD) (Hirosumi et al., 2002). Studies of tissue-specific JNK-deficient mice demonstrate that these obesity and insulin resistance phenotypes can be separated. Thus, JNK regulation of the hypothalamic-pituitary hormone axis that regulates energy expenditure is critically required for the development of diet-induced obesity (Belgardt et al., 2010; Sabio et al., 2010a; Vernia et al., 2013). In contrast, JNK function in peripheral tissues, including fat, muscle, and inflammatory cells contributes to diet-induced insulin resistance (Sabio et al., 2008; Sabio et al., 2010b; Han et al., 2013).

Consuming a HFD increases the blood concentration of free fatty acids (Kahn et al., 2006) and causes JNK activation mediated by the mixed-lineage protein kinase pathway (Jaeschke and Davis, 2007; Kant et al., 2013). Activated JNK contributes to obesity development by increasing Activating Protein 1 (AP1)-dependent *Dio2* gene expression in the anterior pituitary gland (Vernia et al., 2013). In contrast, targets of JNK signaling that cause insulin resistance are unclear. Early studies suggested that phosphorylation of the insulin receptor adapter protein IRS1 by JNK causes insulin resistance (Aguirre et al., 2000), but subsequent studies have not confirmed this conclusion (Copps et al., 2010). More recently, JNK-mediated regulation of adipokines (Sabio et al., 2008) and inflammatory cytokines (Han et al., 2013) has been implicated in the development of insulin resistance. For example, the promotion of hepatic insulin sensitivity caused by JNK-deficiency in adipocytes and myeloid cells is associated with defects in adipokine/cytokine expression (Sabio et al., 2008; Han et al., 2013). These data indicate that JNK-mediated hepatic insulin resistance may be caused by JNK function in non-hepatic cells (Sabio et al., 2008; Han et al., 2013). This conclusion is consistent with the finding that whole body JNK1-deficiency (Hirosumi et al., 2002), but not hepatic JNK1-deficiency (Sabio et al., 2009), protects against HFD-induced insulin resistance. The function of hepatic JNK is therefore unclear.

The purpose of this study was to re-evaluate the role of hepatic JNK in the metabolic stress response caused by the consumption of a HFD. It is established that JNK is encoded by the *Jnk1* and *Jnk2* genes in liver (Davis, 2000). We show that mice with compound hepatic ablation of both genes (*Jnk1* and *Jnk2*) exhibit systemic protection against HFD-induced insulin resistance. Moreover, we demonstrate that the peroxisome proliferator-activated

receptor α (PPAR α) - fibroblast growth factor 21 (FGF21) hormone axis contributes to metabolic regulation by hepatic JNK.

Results

Establishment of mice with JNK-deficiency in the liver

To test the role of hepatic JNK, we compared control mice (L^{WT}) and mice with hepatocyte-specific deficiency of JNK1 (L¹), JNK2 (L²), or JNK1 plus JNK2 (L^{1,2}) (Fig. 1A,B). High fat diet (HFD)-induced JNK activation in the liver of L^{WT} mice was partially suppressed in L¹ and L² mice (Figure 1C). In contrast, hepatic JNK activity was not detected in L^{1,2} mice (Figure 1C). These data indicate that JNK1 and JNK2 may serve partially redundant functions in the liver and confirm the absence of hepatic JNK activity in L^{1,2} mice. We employed these mouse strains to examine the metabolic consequences of hepatic JNK-deficiency.

Hepatic JNK-deficiency reduces diet-induced obesity

We found that hepatic JNK-deficiency caused no change in body mass when mice were fed a chow diet (Figure 1D & S1A,B). Similarly, HFD-fed L^{WT} mice and L¹ mice developed equal obesity (Figure 1D & S1A,B). In contrast, HFD-fed L² mice and L^{1,2} mice gained less fat mass than HFD-fed L^{WT} mice (Figure 1D & S1A,B). These data indicate that JNK2-deficiency, rather than JNK1-deficiency, most closely mimics the phenotype of compound deficiency of JNK1 plus JNK2.

The reduced obesity of L^{1,2} mice compared with L^{WT} mice was associated with reduced adipose tissue mass (Figure S1B), reduced VLDL triglyceride in serum (Figure S1D,E), reduced total serum triglyceride (31.7 ± 0.03 mg/dl compared with 64.8 ± 0.09 mg/dl; mean \pm SEM; n = 8; p < 0.03), reduced hepatic expression of lipogenic genes, including *Srebf1* and *Fasn* (Figure S1F,G), and reduced *de novo* hepatic lipogenesis (Figure S1H). Together, these data demonstrate that hepatic JNK-deficiency causes dysregulated lipid metabolism.

Hepatic JNK-deficiency increases insulin sensitivity

The HFD-fed L^{1,2} mice showed improved tolerance to glucose, insulin, and pyruvate (Figure 1E–G). Hyperinsulinemic-euglycemic clamp studies demonstrated reduced hepatic glucose production, increased hepatic insulin action, improved whole body insulin sensitivity (detected by increased glucose infusion rates during the clamps), and increased whole body glycogen plus lipid synthesis (Figure 1H–K). These data demonstrate that hepatic JNK-deficiency causes protection of mice against HFD-induced insulin resistance.

We performed biochemical studies of insulin signaling by measurement of AKT activation in L^{WT} and L^{1,2} mice. This analysis demonstrated that L^{1,2} mice were partially protected against the HFD-induced suppression of insulin-stimulated AKT activation in liver, adipose tissue, and skeletal muscle that was detected in L^{WT} mice (Fig. 1L–N). These data confirm the conclusion that HFD-fed L^{1,2} mice exhibit a systemic increase in insulin sensitivity compared with L^{WT} mice. The increased insulin sensitivity of L^{1,2} mice correlates with reduced HFD-induced islet hypertrophy, hyperinsulinemia, and suppression of glucose-

stimulated insulin secretion (Figure 2A–D). Moreover, HFD-induced hyperglycemia was significantly suppressed in L^{1,2} mice compared with L^{WT} mice (Figure 2E,F).

The improved insulin sensitivity of HFD-fed L^{1,2} mice contrasts with our previous analysis of L¹ mice with liver-specific JNK1-deficiency that exhibit increased insulin resistance compared with L^{WT} mice (Sabio et al., 2009). This analysis suggests that hepatic JNK2 may play a critical role in glycemic regulation. Indeed, HFD-fed L² mice exhibited increased glucose tolerance, reduced islet hypertrophy, and reduced hyperinsulinemia compared with HFD-fed L^{WT} mice (Figure S2A–F). The HFD-fed L² mice also exhibited increased insulin sensitivity in hyperinsulinemic-euglycemic clamp studies (Figure S2G–M). Nevertheless, these glycemic phenotypes of L² mice (Figure S2) are modest compared with L^{1,2} mice (Figures 1 & 2). Together, these data indicate that L¹ mice and L² mice exhibit different glycemic phenotypes, and that L² mice, and especially L^{1,2} mice, show improved control of blood glucose concentration compared with L^{WT} mice.

The mechanism that accounts for the differential effects of hepatic JNK1 and JNK2 deficiency is unclear. Previous studies have established that isoforms of JNK with different protein kinase activities are derived by alternative splicing of primary transcripts of the *Jnk1* and *Jnk2* genes (Davis, 2000). Indeed, JNK substrate specificity is determined by the mutually exclusive inclusion of exons 7a or 7b in *Jnk1* and *Jnk2* mRNA that encode JNK isoforms α and β (Gupta et al., 1996). Analysis of hepatic *Jnk* mRNA demonstrated that the major JNK isoforms in liver correspond to JNK1 β and JNK2 α (Figure S1C). This pattern of alternative splicing of *Jnk* mRNA may contribute to the differential phenotypes caused by ablation of the hepatic *Jnk1* or *Jnk2* genes.

Hepatic JNK-deficiency increases fatty acid oxidation

Hepatic gene expression in chow-fed and HFD-fed mice was examined using RNA-seq analysis (Figure S3A,B). JNK-deficiency caused increased gene expression in HFD-fed mice (Figure S3C–E). Gene ontology analysis demonstrated that L¹ mice and L² mice were markedly different and that L² mice resembled L^{1,2} mice (Figure S3F–H). Differentially regulated genes that contribute to the hepatic phenotype of the JNK-deficient mice were therefore identified by comparing gene expression patterns with the glycemic phenotype of the mice (L¹ < L^{WT} < L² < L^{1,2}). Genes down-regulated in L¹ mice and up-regulated in L^{1,2} mice to a greater extent than L² mice compared with L^{WT} mice were identified, including *Fgf21* (Figure 3A,B). Gene ontology analysis identified significant ($p_{adj} < 0.001$) association of hepatic JNK1 plus JNK2-deficiency with the PPAR pathway and oxidative metabolism (Figure 3C).

To test whether JNK-deficiency increases oxidative metabolism, we investigated mitochondrial oxygen consumption by L^{1,2} and L^{WT} hepatocytes incubated with different substrates. We found that JNK-deficiency caused increased mitochondrial oxygen consumption in the presence of palmitate (Figure 3D). In contrast, mitochondrial oxygen consumption by L^{1,2} hepatocytes metabolizing glucose or pyruvate/lactate was decreased (Figure 3D). Moreover, glucose production by L^{1,2} hepatocytes metabolizing lactate/pyruvate was increased compared with L^{WT} hepatocytes (Figure 3E). This increase in glucose production *in vitro* was associated with increased expression of the gluconeogenic

genes *G6pc* and *Pck1* by L^{1,2} hepatocytes compared with L^{WT} hepatocytes (Figure S1I). We also found that lactate production by L^{1,2} hepatocytes metabolizing glucose was increased compared with L^{WT} hepatocytes (Figure 3F). These effects of JNK-deficiency were associated with increased expression of citric acid cycle and respiratory chain genes together with increased expression of *Pdk4*, an inhibitor of the oxidative metabolism of pyruvate (Figure 3G). These data demonstrate that JNK-deficiency increases the glycolytic conversion of glucose to lactate and selectively promotes the oxidation of fatty acids.

Hepatic JNK-deficiency activates the PPAR α pathway

The hepatic PPAR α pathway (and PPAR β/δ in fat and muscle) increases fatty acid oxidation by peroxisomes, mitochondria, and the endoplasmic reticulum (Evans et al., 2004; Pyper et al., 2010). PPAR α pathway activation and increased fatty acid oxidation in the liver of L^{1,2} mice are reflected by increased PPAR α target gene expression (Figure S3B), including genes required for β -oxidation in peroxisomes (Figure 3I) and mitochondria (Figure 3J) together with ω -oxidation in the endoplasmic reticulum (Figure 3K) compared with L^{WT} mice. The L^{1,2} mice also exhibited increased numbers of hepatic peroxisomes (Figure 4A,C), increased mitochondrial size (Figure 4B,D,E) (consistent with reduced JNK-promoted mitochondrial fission (Leboucher et al., 2012)), and reduced respiratory exchange ratio (Figure S4) compared with L^{WT} mice. These data are consistent with the presence of increased PPAR α pathway-stimulated fatty acid oxidation in the liver of L^{1,2} mice. The increased fatty acid oxidation (Figure 3D), together with reduced lipogenesis (Figure S1F–H), contributes to the reduced hepatic steatosis detected in L^{1,2} mice compared with L^{WT} mice (Figure 3H). Since treatment with PPAR α agonists can improve glycemia by increasing fatty acid oxidation (Evans et al., 2004; Pyper et al., 2010), PPAR α pathway activation may contribute to the phenotype of L^{1,2} mice (Figures 1 & 2).

The mechanism that mediates PPAR α pathway activation in JNK-deficient liver is unclear. We therefore examined PPAR α -dependent gene expression in primary hepatocytes. Studies of three PPAR α target genes (*Acox1*, *Ehhadh*, and *Pdk4*) demonstrated no major differences in the amount of basal expression between L^{1,2} and L^{WT} hepatocytes. Gene expression was suppressed by treatment with the PPAR α antagonists GW6471 or MK886 (Figure 5A). Treatment with the PPAR α agonists WY14043 or Fenofibrate caused increased gene expression by L^{WT} hepatocytes that was greatly potentiated in L^{1,2} hepatocytes (Figure 5A). This increase in PPAR α -dependent gene expression was not caused by changes in the expression of PPAR α or its heterodimeric partner RXR α (Figure 5B). Reduced expression of co-repressors could contribute to increased PPAR α function (Perissi et al., 2010; Mottis et al., 2013) and previous studies have established that decreased NCoR1 expression can cause increased nuclear hormone receptor activity (Li et al., 2011; Yamamoto et al., 2011). We found that hepatic JNK-deficiency decreased the expression of the PPAR α co-repressors NCoR1 and NRIP1 (Figure 5B,C). The reduced expression of these co-repressors may contribute to the metabolic phenotype of L^{1,2} mice because it is established that reduced expression of NCoR1 (Mottis et al., 2013) or NRIP1 (Nautiyal et al., 2013) is sufficient to promote insulin sensitivity.

To confirm the conclusion that loss of JNK protein kinase activity causes increased PPAR α pathway activity, we examined the effect of the selective inhibitor JNK-in-8 (Zhang et al., 2012). This analysis demonstrated that inhibition of JNK protein kinase activity caused increased PPAR α target gene expression (*Ehhadh*, *Fgf21* & *Pdk4*) by primary hepatocytes treated with the PPAR α -agonist Fenofibrate (Figure 5D). The JNK inhibitor also caused decreased expression of *Ncor1* mRNA (Figure 5D). This observation indicates that the JNK inhibitor and *Jnk* gene ablation cause a similar decrease in *Ncor1* expression and increase in PPAR α pathway activity. However, the decrease in *Nrip1* expression detected in L^{1,2} hepatocytes (Figure 5B,C) was not detected when wild-type hepatocytes were treated with the JNK inhibitor (Figure 5D). The mechanism that accounts for this differential regulation of *Nrip1* expression is unclear, but it is possible that short-term pharmacological JNK inhibition may be insufficient to phenocopy the effects of chronic JNK loss-of-function in L^{1,2} hepatocytes. These data suggest that *Ncor1*, rather than *Nrip1*, represents a key target of hepatic JNK.

To test whether decreased *Ncor1* expression is sufficient to account for PPAR α pathway activation, we used shRNA to knock-down hepatic *Ncor1* expression with an adenovirus-associated virus serotype 8 (AAV8) vector. Control studies demonstrated that the AAV8-sh*Ncor1* vector reduced the expression of hepatic *Ncor1* mRNA (Figure 5E). Expression of PPAR α target genes (*Fgf21* and *Pdk4*) was increased in the mice treated with the AAV8-sh*Ncor1* vector compared with mice treated with the control AAV8-shLuc vector (Figure 5E). These data confirm that reduced NCoR1 expression is sufficient to increase hepatic PPAR α pathway activity.

We performed complementation assays to test whether restoration of NCoR1 expression suppressed the effect of hepatic JNK-deficiency to increase PPAR α target gene expression. Indeed, ectopic NCoR1 expression in the liver of L^{1,2} mice reduced expression of the PPAR α target genes *Acox1*, *Ehhadh*, and *Pdk4* (Figure 5F). Moreover, restoring NCoR1 prevented the effect of JNK-deficiency to cause improved glucose tolerance in HFD-fed mice (Figure 5G). Together, these data confirm the conclusion that reduced NCoR1 expression contributes to the effects of JNK-deficiency on the hepatic PPAR α signaling pathway.

A reduction in co-repressor expression in JNK-deficient hepatocytes (Figure 5B,C) may cause not only increased PPAR α activity, but also increased activity of other nuclear hormone receptors, including the thyroid hormone receptor that binds NCoR1 (Horlein et al., 1995). Indeed, reduced NCoR1 expression in the liver caused increased expression of the thyroid hormone receptor target gene *Dio1* (Figure 5E). To test this prediction, we examined triiodothyronine (T3)-stimulated gene expression in primary hepatocytes isolated from L^{WT} and L^{1,2} mice. We found that JNK-deficiency caused significantly increased T3-stimulated expression of thyroid hormone receptor target genes (Figure S5A). Increased expression of these genes in the liver of L^{1,2} mice compared with L^{WT} mice *in vivo* was detected in the absence of significant changes in the amount of blood thyroid hormone (Figure S5B,C). These data support the conclusion that hepatic JNK-deficiency may increase the activity of multiple nuclear hormone receptors by decreasing co-repressor activity.

Hepatic JNK-deficiency and the PPAR γ pathway

The PPAR γ pathway plays an important role in AP1-dependent regulation of hepatic lipid metabolism (Hasenfuss et al., 2014). The mechanism is mediated by increased expression of PPAR γ 2 that is promoted by cFos heterodimers with cJun/JunB/JunD and is antagonized by Fra1/2 heterodimers with cJun (Hasenfuss et al., 2014). Since AP1 proteins are key targets of the JNK signaling pathway (Davis, 2000), we anticipated that hepatic JNK-deficiency may regulate the expression of both AP1 proteins and PPAR γ 2. Indeed, hepatic JNK-deficiency caused reduced expression of cJun, JunD, Fra2, cFos, and FosB in HFD-fed mice (Figure S6A), but hepatic JNK-deficiency caused no significant change in the HFD-induced expression of PPAR γ 2 (Figure S6B). The absence of a PPAR γ 2 expression phenotype caused by hepatic JNK-deficiency was an unexpected finding that may reflect the balance of positive and negative regulation of PPAR γ 2 expression by different heterodimeric AP1 transcription factor complexes (Hasenfuss et al., 2014). Nevertheless, compromised hepatic AP1 function in L^{1,2} mice (Figure S6A) may contribute to decreased expression of *Ncor1* and *Nrip1* (Figure S6C,D), and indirectly increase PPAR γ pathway activity by reducing co-repressor expression.

Hepatic JNK-deficiency increases expression of the PPAR α target gene *Fgf21*

We performed chromatin immunoprecipitation assays to examine proteins bound to the promoter of the PPAR α target gene *Fgf21* (Figure 6A). This analysis demonstrated that JNK-deficiency increased the amount of PPAR α bound to the *Fgf21* promoter (Figure 6B). We also found that JNK-deficiency reduced the amount of bound NCoR1 (Figure 6C). In contrast, JNK-deficiency did not change the interaction of NRIP1 with the *Fgf21* promoter (Figure 6C). As expected, the reduced interaction with NCoR1 was associated with increased histone acetylation on the *Fgf21* promoter (Figure 6D). Together, these data indicate that reduced NCoR1 function contributes to increased PPAR α pathway activation caused by JNK-deficiency in the liver.

The hepatic PPAR α pathway plays a major role in ketogenesis (Evans et al., 2004; Pyper et al., 2010). The mechanism is mediated, in part, by PPAR α -dependent expression of *Fgf21* (Badman et al., 2007; Inagaki et al., 2007; Badman et al., 2009; Potthoff et al., 2009), a gene that is dysregulated by hepatic JNK-deficiency (Figure 3A). Comparison of L^{WT} and L^{1,2} mice demonstrated that JNK-deficiency caused increased hepatic expression of *Fgf21* mRNA (Figure 6E), increased circulating amounts of FGF21 in the blood (Figure 6F), and increased ketogenesis (Figure 6G). Complementation assays demonstrated that restoration of hepatic NCoR1 expression (Figure 6H) suppressed the effect of JNK-deficiency to cause increased expression of *Fgf21* mRNA in the liver (Figure 6I) and the amount of FGF21 circulating in the blood (Figure 6J). Moreover, shRNA-mediated knock-down of *Ncor1* caused increased hepatic expression of FGF21 (Figure 5E). Together, these data confirm that JNK-regulated NCoR1 expression contributes to the effects of JNK to inhibit the PPAR α - FGF21 hormone axis.

To test whether increased *Fgf21* expression contributes to the phenotype of L^{1,2} mice, we used shRNA to knock-down hepatic *Fgf21* expression. Control studies demonstrated that an AAV8-shFgf21 vector reduced hepatic *Fgf21* mRNA expression by $75 \pm 7\%$ (mean \pm SD; n

= 6; $p < 0.05$). Moreover, the amount of FGF21 in the blood was reduced in mice treated with the AAV8-shFgf21 vector compared with mice treated with the control AAV8-shLuc vector (Figure 7A). We found that the *shFgf21* vector prevented the increased ketogenesis (Figure 7B) and suppressed the improved insulin tolerance (Figure 7C) caused by hepatic JNK-deficiency. These data support the conclusion that the PPAR α - FGF21 hormone axis contributes to metabolic regulation by hepatic JNK.

FGF21 contributes to the systemic metabolic effects of hepatic JNK-deficiency

FGF21 regulates adipose tissue metabolism, in part, by reducing PPAR γ inhibitory sumoylation (Dutchak et al., 2012) and increasing PGC1 α expression (Potthoff et al., 2009; Fisher et al., 2012). We therefore examined L^{WT} and L^{1,2} mice to investigate whether hepatic JNK might regulate a FGF21/PPAR γ - PGC1 α axis in adipose tissue. Analysis of epididymal adipose tissue sections demonstrated that the HFD-induced hypertrophy and macrophage infiltration of L^{WT} adipose tissue were reduced in L^{1,2} mice (Figure S7A). Gene expression analysis demonstrated decreased expression of macrophage genes, including genes associated with both M1 and M2 polarization, and reduced expression of the adipokine Leptin (Figure S7B). These observations are consistent with the decreased obesity of HFD-fed L^{1,2} mice compared with HFD-fed L^{WT} mice (Figure 1D & S1A,B). We found that L^{1,2} mice exhibited increased expression of the adipose tissue PPAR γ target genes *Adiponectin* (Holland et al., 2013; Lin et al., 2013) and *Fgf21* (Muisse et al., 2008; Wang et al., 2008) compared with L^{WT} mice (Figure S7B). FGF21-stimulated *Pgc1 α* expression has been implicated in the brown-like adaptation of sub-cutaneous white adipose tissue (Fisher et al., 2012). Indeed, we found increased expression of brown-like genes in the inguinal adipose tissue of HFD-fed L^{1,2} mice compared with HFD-fed L^{WT} mice (Figure S7C). Together, these data indicate that FGF21 contributes to the systemic metabolic effects of hepatic JNK-deficiency.

Discussion

The liver is a critical organ that orchestrates metabolism within the body. In the fed state, hepatic lipogenesis is increased and the liver can export triglycerides in the form of very low density lipoprotein to peripheral tissues. In contrast, fasting increases hepatic fatty acid oxidation and the delivery of ketone bodies to peripheral tissues. The re-programming of liver function between these two metabolic states is mediated, in part, by endocrine hormones (insulin, glucagon, FGF15/19, and FGF21) (Potthoff et al., 2012). The metabolic transition also involves key signal transduction pathways that are differentially activated during feeding and starvation. For example, the PPAR α pathway plays an important role during starvation by increasing fatty acid oxidation / ketogenesis and promoting insulin sensitivity (Evans et al., 2004; Pyper et al., 2010). In contrast, the cJun NH₂-terminal kinase (JNK) signaling pathway is active in the fed state and is implicated in hepatic steatosis and insulin resistance (Davis, 2000; Sabio and Davis, 2010). These opposing actions of the PPAR α and JNK signaling pathways contribute to a metabolic switch that can determine liver function.

This study demonstrates that JNK plays a major role in the regulation of hepatic metabolism by inhibiting nuclear hormone receptor pathways, including PPAR α , that increase fatty acid oxidation and ketogenesis. Multiple PPAR α target genes likely contribute to these actions of JNK, but *Fgf21* plays a key role in ketogenesis (Badman et al., 2007; Badman et al., 2009), insulin sensitivity (Holland et al., 2013; Lin et al., 2013), glycemia (Kharitonov et al., 2005; Xu et al., 2009a; Xu et al., 2009b), and obesity (Kharitonov et al., 2005; Coskun et al., 2008). Indeed, suppression of FGF21 expression in the liver prevents the effects of hepatic JNK-deficiency on insulin sensitivity and ketogenesis (Figure 7). The PPAR α - FGF21 hormone axis is therefore an important target of the hepatic JNK signaling pathway that regulates metabolism.

Our analysis establishes that JNK inhibits PPAR α target gene expression in the liver. This effect of JNK is not mediated by changes in the expression of PPAR α (or its partner RXR α), but is associated with reduced expression of the co-repressors NCoR1 and NRIP1 (Figure 5B,C). ChIP assays demonstrated that JNK-deficiency changes the interaction of PPAR α (increased) and NCoR1 (reduced) with a PPRE in the promoter of the PPAR α target gene *Fgf21* (Figure 6A–C). This reduction in co-repressor binding is sufficient to account for PPAR α pathway activation (Perissi et al., 2010; Mottis et al., 2013) and may be caused by the reduced co-repressor expression detected in mice with hepatic JNK-deficiency (Figure 5B,C). Indeed, shRNA studies demonstrated that *Ncor1* knock-down was sufficient to cause increased hepatic FGF21 expression (Figure 5E). Moreover, restoration of *Ncor1* expression in the liver prevented PPAR α pathway activation (Figure 5F), FGF21 expression (Figure 6I,J), and improved glucose tolerance (Figure 5G) caused by JNK-deficiency. These data demonstrate that JNK promotes repression of PPAR α target gene expression by regulating co-repressor function.

The presence of AP1 sites in the *Ncor1* and *Nrip1* promoters (Figure S6C,D) suggests that these genes may be direct targets of a hepatic JNK signaling pathway that activates AP1 (Figure S6A), but other transcription factors or indirect mechanisms (e.g. miRNA pathways) may also contribute to JNK-regulated expression of NCoR1 and NRIP1. Additional analysis will be required to define the mechanism of co-repressor regulation by hepatic JNK. Nevertheless, it is established that *Ncor1* mRNA expression is dynamically regulated by exposure of cells to fatty acids and other stimuli that can activate JNK (Yamamoto et al., 2011). Indeed, JNK-stimulated *Ncor1* gene expression may contribute to this dynamic regulation and cause JNK-mediated repression of the PPAR α pathway.

Further studies will be required to test whether PPAR α pathway repression is mediated exclusively by JNK-regulated expression of the co-repressors NCoR1 and NRIP1. Our analysis does not exclude the possibility that additional factors may contribute to co-repressor regulation. Examples include roles for alternative splicing, phosphorylation, nuclear/cytoplasmic transport, protein stability (sumoylation), and protein instability (ubiquitination) (Perissi et al., 2010; Mottis et al., 2013). The possible regulation of NCoR1 degradation by JNK is intriguing because studies of AP1 regulation in macrophages have established that cJun phosphorylation triggers the dissociation and subsequent degradation of NCoR1 (Ogawa et al., 2004). Whether this mechanism is relevant to the PPAR α pathway is unclear. Nevertheless, a recent study has highlighted NCoR1 protein turnover as an

important regulatory mechanism for gene expression related to energy metabolism (Catic et al., 2013).

The regulation of NCoR1 and NR1P1 expression by JNK suggests that mice with hepatic JNK-deficiency may exhibit altered function of multiple nuclear receptors. For example, hepatic NCoR1 functions as a potent inhibitor of thyroid hormone signaling (Feng et al., 2001; Astapova et al., 2008; Fozzatti et al., 2011) and we found that hepatic JNK-deficiency caused increased thyroid hormone-dependent gene expression (Figure S5). Similarly, both NCoR1 and NR1P1 inhibit the nuclear hormone receptor LXR (Herzog et al., 2007; Astapova et al., 2008). JNK-deficiency may therefore also regulate LXR, cross-talk with the PPAR α pathway (Boergesen et al., 2012), and contribute to the regulation of hepatic lipid metabolism (Beaven et al., 2013). These considerations indicate that there is potential for significant complexity in the hepatic nuclear receptor signaling network that is regulated by JNK. Further studies will be required to determine the roles of these nuclear receptors (including FXR, GR, HNF4, LXR & TR) in the metabolic response to JNK activation. Nevertheless, our analysis establishes that the PPAR α -FGF21 hormone axis is an important mediator of metabolic regulation by hepatic JNK.

Conclusions

The activity of hepatic JNK is regulated by starvation and feeding. These changes in JNK activity regulate the hepatic PPAR α - FGF21 hormone axis. Studies of mice with hepatic JNK-deficiency demonstrate an exaggerated starvation response (increased ketogenesis) and a reduced response to feeding (protection against hyperglycemia and insulin resistance). These responses are mediated, in part, by the hepatic PPAR α - FGF21 hormone axis. Hepatic JNK therefore plays a key role in diet-mediated metabolic regulation.

EXPERIMENTAL PROCEDURES

Mice

We have previously described $Jnk1^{LoxP/LoxP}$ mice (Das et al., 2007) and $Jnk2^{LoxP/LoxP}$ mice (Han et al., 2013). C56BL/6J mice (stock number 000664), and B6.Cg-Tg(Alb-cre)21Mgn/J mice (stock number 003574) (Postic et al., 1999) were obtained from The Jackson Laboratory. The mice were backcrossed to the C57BL/6J strain (ten generations) and housed in a facility accredited by the American Association for Laboratory Animal Care (AALAC). The mice employed in this study were L^{WT} (Cre^+), L^1 ($Cre^+ Jnk1^{LoxP/LoxP}$), L^2 ($Cre^+ Jnk2^{LoxP/LoxP}$), and $L^{1,2}$ ($Cre^+ Jnk1^{LoxP/LoxP} Jnk2^{LoxP/LoxP}$). All studies were performed using male mice (8–24 wk old). Male mice (8 weeks old) were fed a standard Control (chow) diet or a high fat diet (HFD) (Iso Pro 3000, Purina and F3282, Bioserve, Inc.). Whole body fat and lean mass were non-invasively measured using 1H -MRS (Echo Medical Systems). The animal studies were approved by the Institutional Animal Care and Use Committee of the University of Massachusetts Medical School.

Viral transduction studies

The adeno-associated virus (AAV) vector pAAVscCB6siFluc EGFP that expresses an shRNA that targets Luciferase was modified by exchanging the Luciferase shRNA sequence

(*Bam*H1 sites) with a sequence that encodes an *Fgf21* shRNA (5'-GATCAAAAAAGGGATTCAACACAG GAGAAACTTCGGTTTCTCCTGTGTTGAATCCC-3'). The vector pAAV-RFP-U6 used to express *Ncor1* shRNA (target sequence 5'-CGGCATAATCTTGACAACCTT-3') was obtained from Vector Biolabs. Recombinant AAV serotype 8 (AAV8) were prepared and amplified by the University of Massachusetts Gene Therapy Vector Core (Mueller et al., 2012; Ahmed et al., 2013). Male mice (8 weeks old) were treated by intravenous injection (tail vein) with 3×10^{11} genomic copies/mouse of AAV8-*shLuc* (Control), AAV8-*shFgf21*, or AAV8-*shNcor1* (200 μ l final volume). Studies were performed 30 ~ 90 days post-infection.

Complementation studies were performed using Ad-GFP (Control) and Ad-NcoR1 (NM_001252313) adenovirus stocks obtained from Applied Biological Materials. Male mice (8 weeks old) were fed a HFD (4 wks.) and then treated by intravenous injection (tail vein; 200 μ l final volume) with 8×10^9 genomic copies/mouse of recombinant adenovirus. Studies were performed 10 ~ 16 days post-infection.

Blood analysis

Blood glucose was measured with an Ascensia Breeze 2 glucometer (Bayer). β -Hydroxybutyrate was measured by colorimetric assays (Wako). Insulin and TSH in plasma were measured by multiplexed ELISA using a Luminex 200 machine (Millipore). T3 and T4 (Calbiotech) and FGF21 (Millipore) in plasma were measured using ELISA kits. Serum triglyceride was measured using a kit (Sigma). Lipoprotein analysis was performed by the University of Cincinnati Mouse Metabolic Phenotyping Center.

Glucose, insulin and pyruvate tolerance tests

Glucose and insulin tolerance tests were performed by intraperitoneal injection of mice with glucose (1g/kg), insulin (0.5 U/kg) or pyruvate (1g/kg) using methods described previously (Sabio et al., 2008).

Hepatic lipogenesis

Mice were starved overnight and re-fed (3h). Lipogenesis was examined *in vivo* by injecting mice with 20 μ Ci/g $^3\text{H}_2\text{O}$ and measurement of radioactivity incorporation by scintillation counting with adjustments for $^3\text{H}_2\text{O}$ specific activity and tissue mass (Stansbie et al., 1976; Zhang et al., 2006).

Ketogenesis assays

Ketone body formation *in vivo* was measured using the ketogenic substrate octanoate (McGarry and Foster, 1971). Briefly, mice starved overnight were subjected to intraperitoneal injection of 10 μ L/g of 250 mM sodium octanoate in sterile water prior to measurement of β -hydroxybutyrate in the blood (Potthoff et al., 2009).

Hyperinsulinemic-euglycemic clamp studies

The clamp studies were performed by the UMASS Mouse Metabolic Phenotyping Center. Following an overnight fast, a 2-hr hyperinsulinemic-euglycemic clamp was conducted in conscious mice with a primed and continuous infusion of human insulin (150 mU/kg body weight priming followed by 2.5 mU/kg/min; Humulin; Eli Lilly), and 20% glucose was infused at variable rates to maintain euglycemia (Kim et al., 2004).

Metabolic cage analysis

The analysis was performed by the Mouse Metabolic Phenotyping Center at the University of Massachusetts Medical School. The mice were housed under controlled temperature and lighting with free access to food and water using metabolic cages (TSE Systems).

Statistical analysis

Differences between groups were examined for statistical significance using the Student's test or analysis of variance (ANOVA) with the Fisher's test.

Supplementary Material

Refer to Web version on PubMed Central for supplementary material.

Acknowledgments

We thank Alfredo Giménez-Cassina and Marc Liesa for critical discussions, Shmulik Motola for assistance with RNA-seq analysis, Lara Strittmatter and Greg Hendricks for assistance with electron microscopy, Vicky Benoit for expert technical assistance, and Kathy Gemme for administrative assistance. These studies were supported by a grant from the National Institutes of Health (DK090963). The UMASS Mouse Metabolic Phenotyping Center is supported by grant DK093000. The UMASS Electron Microscopy Core is supported by grants from the National Center For Research Resources (S10RR021043 and S10RR027897). G.S. was supported by the Ramón y Cajal Program and grants ERC 260464, EFSO 2030, MICINN SAF2010-19347 and Comunidad de Madrid S2010/BMD-2326. CNIC is supported by the Ministry of Economy and Competitiveness and the Pro-CNIC Foundation. S.V. was supported by a fellowship from the Ramon Areces Foundation. R.J.D. is an Investigator of the Howard Hughes Medical Institute.

References

- Aguirre V, Uchida T, Yenush L, Davis R, White MF. The c-Jun NH(2)-terminal kinase promotes insulin resistance during association with insulin receptor substrate-1 and phosphorylation of Ser(307). *J Biol Chem.* 2000; 275:9047–9054. [PubMed: 10722755]
- Ahmed SS, Li J, Godwin J, Gao G, Zhong L. Gene transfer in the liver using recombinant adeno-associated virus. *Curr Prot Micro.* 2013; Chapter 14(Unit14D):16.
- Astapova I, Lee LJ, Morales C, Tauber S, Bilban M, Hollenberg AN. The nuclear corepressor, NCoR, regulates thyroid hormone action in vivo. *Proc Natl Acad Sci USA.* 2008; 105:19544–19549. [PubMed: 19052228]
- Badman MK, Koester A, Flier JS, Kharitonov A, Maratos-Flier E. Fibroblast growth factor 21-deficient mice demonstrate impaired adaptation to ketosis. *Endocrinol.* 2009; 150:4931–4940.
- Badman MK, Pissios P, Kennedy AR, Koukos G, Flier JS, Maratos-Flier E. Hepatic fibroblast growth factor 21 is regulated by PPAR α and is a key mediator of hepatic lipid metabolism in ketotic states. *Cell Metab.* 2007; 5:426–437. [PubMed: 17550778]
- Beaven SW, Matveyenko A, Wroblewski K, Chao L, Wilpitz D, Hsu TW, Lentz J, Drew B, Hevener AL, Tontonoz P. Reciprocal regulation of hepatic and adipose lipogenesis by liver X receptors in obesity and insulin resistance. *Cell Metab.* 2013; 18:106–117. [PubMed: 23823481]

- Belgardt BF, Mauer J, Wunderlich FT, Ernst MB, Pal M, Spohn G, Bronneke HS, Brodesser S, Hampel B, Schauss AC, et al. Hypothalamic and pituitary c-Jun N-terminal kinase 1 signaling coordinately regulates glucose metabolism. *Proc Natl Acad Sci USA*. 2010; 107:6028–6033. [PubMed: 20231445]
- Boergesen M, Pedersen TA, Gross B, van Heeringen SJ, Hagenbeek D, Bindsboll C, Caron S, Lalloyer F, Steffensen KR, Nebb HI, et al. Genome-wide profiling of liver X receptor, retinoid X receptor, and peroxisome proliferator-activated receptor α in mouse liver reveals extensive sharing of binding sites. *Mol Cell Biol*. 2012; 32:852–867. [PubMed: 22158963]
- Catic A, Suh CY, Hill CT, Daheron L, Henkel T, Orford KW, Dombkowski DM, Liu T, Liu XS, Scadden DT. Genome-wide map of nuclear protein degradation shows NCoR1 turnover as a key to mitochondrial gene regulation. *Cell*. 2013; 155:1380–1395. [PubMed: 24315104]
- Copps KD, Hancer NJ, Opere-Ado L, Qiu W, Walsh C, White MF. Irs1 serine 307 promotes insulin sensitivity in mice. *Cell Metab*. 2010; 11:84–92. [PubMed: 20074531]
- Coskun T, Bina HA, Schneider MA, Dunbar JD, Hu CC, Chen Y, Moller DE, Kharitonov A. Fibroblast growth factor 21 corrects obesity in mice. *Endocrinol*. 2008; 149:6018–6027.
- Das M, Jiang F, Sluss HK, Zhang C, Shokat KM, Flavell RA, Davis RJ. Suppression of p53-dependent senescence by the JNK signal transduction pathway. *Proc Natl Acad Sci USA*. 2007; 104:15759–15764. [PubMed: 17893331]
- Davis RJ. Signal transduction by the JNK group of MAP kinases. *Cell*. 2000; 103:239–252. [PubMed: 11057897]
- Dutchak PA, Katafuchi T, Bookout AL, Choi JH, Yu RT, Mangelsdorf DJ, Kliewer SA. Fibroblast growth factor-21 regulates PPAR γ activity and the antidiabetic actions of thiazolidinediones. *Cell*. 2012; 148:556–567. [PubMed: 22304921]
- Evans RM, Barish GD, Wang YX. PPARs and the complex journey to obesity. *Nat Med*. 2004; 10:355–361. [PubMed: 15057233]
- Feng X, Jiang Y, Meltzer P, Yen PM. Transgenic targeting of a dominant negative corepressor to liver blocks basal repression by thyroid hormone receptor and increases cell proliferation. *J Biol Chem*. 2001; 276:15066–15072. [PubMed: 11328825]
- Fisher FM, Kleiner S, Douris N, Fox EC, Mepani RJ, Verdeguer F, Wu J, Kharitonov A, Flier JS, Maratos-Flier E, et al. FGF21 regulates PGC-1 α and browning of white adipose tissues in adaptive thermogenesis. *Genes Dev*. 2012; 26:271–281. [PubMed: 22302939]
- Fozzatti L, Lu C, Kim DW, Park JW, Astapova I, Gavrilova O, Willingham MC, Hollenberg AN, Cheng SY. Resistance to thyroid hormone is modulated in vivo by the nuclear receptor corepressor (NCOR1). *Proc Natl Acad Sci USA*. 2011; 108:17462–17467. [PubMed: 21987803]
- Gupta S, Barrett T, Whitmarsh AJ, Cavanagh J, Sluss HK, Derijard B, Davis RJ. Selective interaction of JNK protein kinase isoforms with transcription factors. *EMBO J*. 1996; 15:2760–2770. [PubMed: 8654373]
- Han MS, Jung DY, Morel C, Lakhani SA, Kim JK, Flavell RA, Davis RJ. JNK expression by macrophages promotes obesity-induced insulin resistance and inflammation. *Science*. 2013; 339:218–222. [PubMed: 23223452]
- Hasenfuss SC, Bakiri L, Thomsen MK, Williams EG, Auwerx J, Wagner EF. Regulation of steatohepatitis and PPAR γ signaling by distinct AP-1 dimers. *Cell Metab*. 2014; 19:84–95. [PubMed: 24411941]
- Herzog B, Hallberg M, Seth A, Woods A, White R, Parker MG. The nuclear receptor cofactor, receptor-interacting protein 140, is required for the regulation of hepatic lipid and glucose metabolism by liver X receptor. *Mol Endocrinol*. 2007; 21:2687–2697. [PubMed: 17684114]
- Hirosumi J, Tuncman G, Chang L, Gorgun CZ, Uysal KT, Maeda K, Karin M, Hotamisligil GS. A central role for JNK in obesity and insulin resistance. *Nature*. 2002; 420:333–336. [PubMed: 12447443]
- Holland WL, Adams AC, Brozinick JT, Bui HH, Miyauchi Y, Kusminski CM, Bauer SM, Wade M, Singhal E, Cheng CC, et al. An FGF21-Adiponectin-Ceramide axis controls energy expenditure and insulin action in mice. *Cell Metab*. 2013; 17:790–797. [PubMed: 23663742]

- Horlein AJ, Naar AM, Heinzl T, Torchia J, Gloss B, Kurokawa R, Ryan A, Kamei Y, Soderstrom M, Glass CK, et al. Ligand-independent repression by the thyroid hormone receptor mediated by a nuclear receptor co-repressor. *Nature*. 1995; 377:397–404. [PubMed: 7566114]
- Inagaki T, Dutchak P, Zhao G, Ding X, Gautron L, Parameswara V, Li Y, Goetz R, Mohammadi M, Esser V, et al. Endocrine regulation of the fasting response by PPARalpha-mediated induction of fibroblast growth factor 21. *Cell Metab*. 2007; 5:415–425. [PubMed: 17550777]
- Jaeschke A, Davis RJ. Metabolic stress signaling mediated by mixed-lineage kinases. *Mol Cell*. 2007; 27:498–508. [PubMed: 17679097]
- Kahn SE, Hull RL, Utzschneider KM. Mechanisms linking obesity to insulin resistance and type 2 diabetes. *Nature*. 2006; 444:840–846. [PubMed: 17167471]
- Kant S, Barrett T, Vertii A, Noh YH, Jung DY, Kim JK, Davis RJ. Role of the mixed-lineage protein kinase pathway in the metabolic stress response to obesity. *Cell reports*. 2013; 4:681–688. [PubMed: 23954791]
- Kharitonov A, Shiyanova TL, Koester A, Ford AM, Micanovic R, Galbreath EJ, Sandusky GE, Hammond LJ, Moyers JS, Owens RA, et al. FGF-21 as a novel metabolic regulator. *J Clin Invest*. 2005; 115:1627–1635. [PubMed: 15902306]
- Kim HJ, Higashimori T, Park SY, Choi H, Dong J, Kim YJ, Noh HL, Cho YR, Cline G, Kim YB, et al. Differential effects of interleukin-6 and -10 on skeletal muscle and liver insulin action in vivo. *Diabetes*. 2004; 53:1060–1067. [PubMed: 15047622]
- Leboucher GP, Tsai YC, Yang M, Shaw KC, Zhou M, Veenstra TD, Glickman MH, Weissman AM. Stress-induced phosphorylation and proteasomal degradation of mitofusin 2 facilitates mitochondrial fragmentation and apoptosis. *Mol Cell*. 2012; 47:547–557. [PubMed: 22748923]
- Li P, Fan W, Xu J, Lu M, Yamamoto H, Auwerx J, Sears DD, Talukdar S, Oh D, Chen A, et al. Adipocyte NCoR knockout decreases PPARgamma phosphorylation and enhances PPARgamma activity and insulin sensitivity. *Cell*. 2011; 147:815–826. [PubMed: 22078880]
- Lin Z, Tian H, Lam KS, Lin S, Hoo RC, Konishi M, Itoh N, Wang Y, Bornstein SR, Xu A, et al. Adiponectin Mediates the Metabolic Effects of FGF21 on Glucose Homeostasis and Insulin Sensitivity in Mice. *Cell Metab*. 2013; 17:779–789. [PubMed: 23663741]
- McGarry JD, Foster DW. The regulation of ketogenesis from octanoic acid. The role of the tricarboxylic acid cycle and fatty acid synthesis. *J Biol Chem*. 1971; 246:1149–1159. [PubMed: 5543682]
- Mottis A, Mouchiroud L, Auwerx J. Emerging roles of the corepressors NCoR1 and SMRT in homeostasis. *Genes Dev*. 2013; 27:819–835. [PubMed: 23630073]
- Mueller C, Ratner D, Zhong L, Esteves-Sena M, Gao G. Production and discovery of novel recombinant adeno-associated viral vectors. *Curr Prot Micro*. 2012; Chapter 14(Unit14D):11.
- Muise ES, Azzolina B, Kuo DW, El-Sherbeini M, Tan Y, Yuan X, Mu J, Thompson JR, Berger JP, Wong KK. Adipose fibroblast growth factor 21 is upregulated by peroxisome proliferator-activated receptor gamma and altered metabolic states. *Mol Pharmacol*. 2008; 74:403–412. [PubMed: 18467542]
- Nautiyal J, Christian M, Parker MG. Distinct functions for RIP140 in development, inflammation, and metabolism. *Trends Endocrinol & Metab*. 2013; 24:451–459. [PubMed: 23742741]
- Ogawa S, Lozach J, Jepsen K, Sawka-Verhelle D, Perissi V, Sasik R, Rose DW, Johnson RS, Rosenfeld MG, Glass CK. A nuclear receptor corepressor transcriptional checkpoint controlling activator protein 1-dependent gene networks required for macrophage activation. *Proc Natl Acad Sci USA*. 2004; 101:14461–14466. [PubMed: 15452344]
- Perissi V, Jepsen K, Glass CK, Rosenfeld MG. Deconstructing repression: evolving models of co-repressor action. *Nat Rev Genet*. 2010; 11:109–123. [PubMed: 20084085]
- Postic C, Shiota M, Niswender KD, Jetton TL, Chen Y, Moates JM, Shelton KD, Lindner J, Cherrington AD, Magnuson MA. Dual roles for glucokinase in glucose homeostasis as determined by liver and pancreatic beta cell-specific gene knock-outs using Cre recombinase. *J Biol Chem*. 1999; 274:305–315. [PubMed: 9867845]
- Pothhoff MJ, Inagaki T, Satapati S, Ding X, He T, Goetz R, Mohammadi M, Finck BN, Mangelsdorf DJ, Kliewer SA, et al. FGF21 induces PGC-1 α and regulates carbohydrate and fatty acid

- metabolism during the adaptive starvation response. *Proc Natl Acad Sci USA*. 2009; 106:10853–10858. [PubMed: 19541642]
- Potthoff MJ, Kliewer SA, Mangelsdorf DJ. Endocrine fibroblast growth factors 15/19 and 21: from feast to famine. *Genes Dev*. 2012; 26:312–324. [PubMed: 22302876]
- Pyper SR, Viswakarma N, Yu S, Reddy JK. PPARalpha: energy combustion, hypolipidemia, inflammation and cancer. *Nuc Recept Signal*. 2010; 8:e002.
- Sabio G, Cavanagh-Kyros J, Barrett T, Jung DY, Ko HJ, Ong H, Morel C, Mora A, Reilly J, Kim JK, et al. Role of the hypothalamic-pituitary-thyroid axis in metabolic regulation by JNK1. *Genes Dev*. 2010a; 24:256–264. [PubMed: 20080940]
- Sabio G, Cavanagh-Kyros J, Ko HJ, Jung DY, Gray S, Jun JY, Barrett T, Mora A, Kim JK, Davis RJ. Prevention of steatosis by hepatic JNK1. *Cell Metab*. 2009; 10:491–498. [PubMed: 19945406]
- Sabio G, Das M, Mora A, Zhang Z, Jun JY, Ko HJ, Barrett T, Kim JK, Davis RJ. A stress signaling pathway in adipose tissue regulates hepatic insulin resistance. *Science*. 2008; 322:1539–1543. [PubMed: 19056984]
- Sabio G, Davis RJ. c-Jun NH2-terminal kinase 1 (JNK1): roles in metabolic regulation of insulin resistance. *Trends Biochem Sci*. 2010; 35:490–496. [PubMed: 20452774]
- Sabio G, Kennedy NJ, Cavanagh-Kyros J, Jung DY, Ko HJ, Ong H, Barrett T, Kim JK, Davis RJ. Role of muscle c-Jun NH2-terminal kinase 1 in obesity-induced insulin resistance. *Mol Cell Biol*. 2010b; 30:106–115. [PubMed: 19841069]
- Stansbie D, Brownsey RW, Crettaz M, Denton RM. Acute effects in vivo of anti-insulin serum on rates of fatty acid synthesis and activities of acetyl-coenzyme A carboxylase and pyruvate dehydrogenase in liver and epididymal adipose tissue of fed rats. *Biochem J*. 1976; 160:413–416. [PubMed: 12755]
- Vernia S, Cavanagh-Kyros J, Barrett T, Jung DY, Kim JK, Davis RJ. Diet-induced obesity mediated by the JNK/DIO2 signal transduction pathway. *Genes Dev*. 2013; 27:2345–2355. [PubMed: 24186979]
- Wang H, Qiang L, Farmer SR. Identification of a domain within peroxisome proliferator-activated receptor gamma regulating expression of a group of genes containing fibroblast growth factor 21 that are selectively repressed by SIRT1 in adipocytes. *Mol Cell Biol*. 2008; 28:188–200. [PubMed: 17954559]
- Xu J, Lloyd DJ, Hale C, Stanislaus S, Chen M, Sivits G, Vonderfecht S, Hecht R, Li YS, Lindberg RA, et al. Fibroblast growth factor 21 reverses hepatic steatosis, increases energy expenditure, and improves insulin sensitivity in diet-induced obese mice. *Diabetes*. 2009a; 58:250–259. [PubMed: 18840786]
- Xu J, Stanislaus S, Chinookoswong N, Lau YY, Hager T, Patel J, Ge H, Weiszmann J, Lu SC, Graham M, et al. Acute glucose-lowering and insulin-sensitizing action of FGF21 in insulin-resistant mouse models--association with liver and adipose tissue effects. *Am J Physiol Endocrinol & Metab*. 2009b; 297:E1105–1114. [PubMed: 19706786]
- Yamamoto H, Williams EG, Mouchiroud L, Canto C, Fan W, Downes M, Heligon C, Barish GD, Desvergne B, Evans RM, et al. NCoR1 is a conserved physiological modulator of muscle mass and oxidative function. *Cell*. 2011; 147:827–839. [PubMed: 22078881]
- Zhang T, Inesta-Vaquera F, Niepel M, Zhang J, Ficarro SB, Machleidt T, Xie T, Marto JA, Kim N, Sim T, et al. Discovery of potent and selective covalent inhibitors of JNK. *Chem Biol*. 2012; 19:140–154. [PubMed: 22284361]
- Zhang W, Patil S, Chauhan B, Guo S, Powell DR, Le J, Klotsas A, Matika R, Xiao X, Franks R, et al. FoxO1 regulates multiple metabolic pathways in the liver: effects on gluconeogenic, glycolytic, and lipogenic gene expression. *J Biol Chem*. 2006; 281:10105–10117. [PubMed: 16492665]

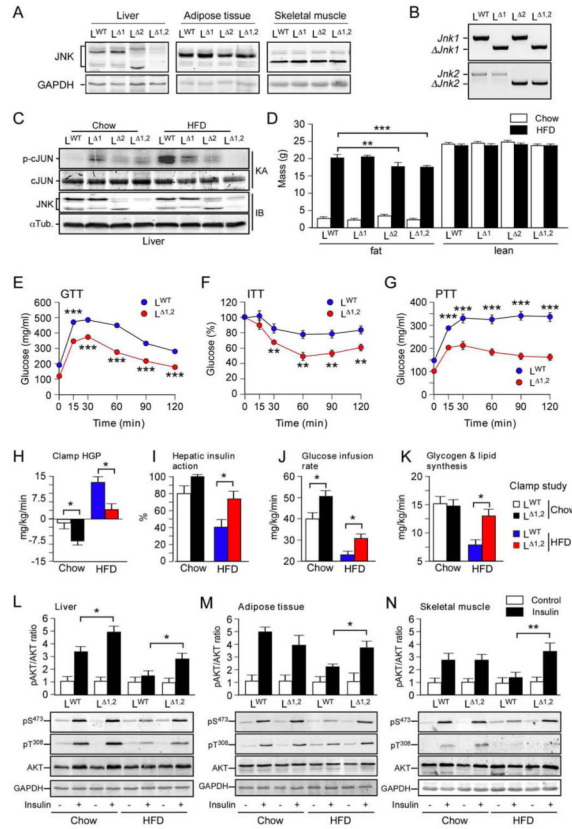


Figure 1. Hepatic JNK contributes to diet-induced obesity and insulin resistance

(A) The liver, adipose tissue (epididymal), and skeletal muscle (gastrocnemius) of L^{WT} , L^1 , L^2 and $L^{1,2}$ mice were examined by immunoblot analysis by probing with antibodies to JNK and GAPDH.

(B) Genomic DNA isolated from the liver of L^{WT} , L^1 , L^2 and $L^{1,2}$ mice was examined by PCR analysis to detect *Jnk* and *Jnk2* alleles.

(C) Liver extracts prepared from mice fed a chow diet or a HFD (16 wk) and starved overnight were examined by immunoblot (IB) analysis by probing with antibodies to α Tubulin and JNK. *In vitro* protein kinase assays (KA) with the substrates GST-cJun and [γ - 32 P]ATP were performed to measure JNK activity. The amount of cJun and phosphorylated cJun (p-cJun) were detected by staining with Coomassie blue and Phosphorimager (Applied Biosystems) analysis, respectively.

(D) The fat and lean mass of chow-fed and HFD-fed (16 weeks) mice were measured by 1 H-MRS analysis (mean \pm SEM; n = 8 ~ 10). Significant differences between L^{WT} and $L^{1,2}$ mice were detected (**, $p < 0.01$, ***, $p < 0.001$).

(E,F) Glucose (GTT) and insulin (ITT) tolerance tests were performed on mice fed (16 wk) a HFD (mean \pm SEM; n = 35 ~ 50; **, $p < 0.01$; ***, $p < 0.001$).

(G) Pyruvate (PTT) tolerance tests were performed on mice fed (16 wk) a HFD (mean \pm SEM; n = 20 ~ 30; *, ***, $p < 0.001$).

(H–K) Insulin sensitivity was measured using hyperinsulinemic-euglycemic clamps with conscious L^{WT} and $L^{1,2}$ mice fed a chow diet or HFD. The hepatic glucose production (HGP) during the clamp, hepatic insulin action (expressed as insulin-mediated percent

suppression of basal HGP), glucose infusion rate, and glycogen plus lipid synthesis (mean \pm SEM for 6 ~ 8 experiments) are presented. Statistically significant differences between L^{WT} and L^{1,2} mice are indicated (* $p < 0.05$).

(L–N) Chow-fed or HFD-fed L^{WT} and L^{1,2} mice were starved overnight and then administered insulin (1.5U/kg body mass) by intraperitoneal injection. Liver, epididymal adipose tissue, and gastrocnemius muscle extracts (prepared 15 mins post-injection) were examined (*upper panels*) by multiplexed ELISA for pS⁴⁷³-AKT and AKT (mean \pm SEM; $n = 5 \sim 6$; *, $p < 0.05$). Representative extracts were also examined by immunoblot analysis using antibodies to AKT, phospho-AKT (pSer⁴⁷³ and pThr³⁰⁸) and GAPDH (*lower panels*). See also Figures S1 & S2.

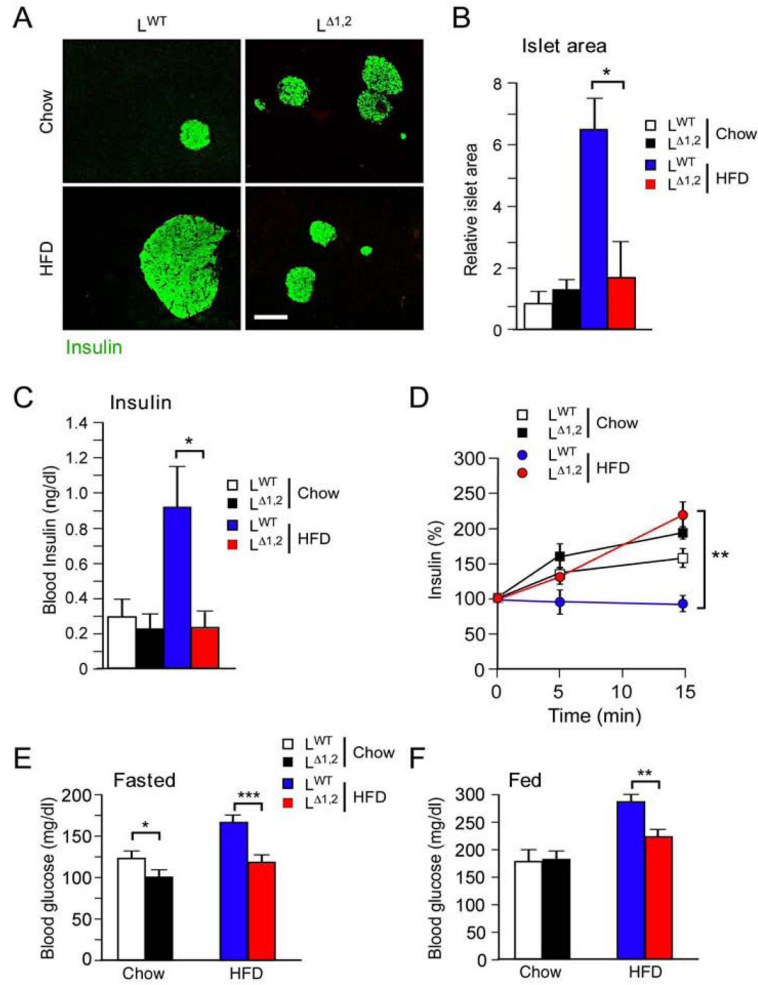


Figure 2. Effect of liver-specific JNK-deficiency on hyperinsulinemia

(A) Mice were fed a chow diet or a HFD (16 wk). Sections of the pancreas were stained with an antibody to insulin. Bar, 100 μ m.

(B) Relative islet size was measured using Image J64 software (mean \pm SEM; n = 30; *, $p < 0.05$).

(C) The mice were fasted overnight and the blood concentration of insulin was measured (mean \pm SEM; n = 16; *, $p < 0.05$).

(D) Glucose-induced insulin secretion was examined using overnight fasted mice by intraperitoneal injection of glucose and measurement of blood insulin concentration (mean \pm SEM; n = 8 ~ 10; **, $p < 0.01$).

(E,F) Mice were fed a chow diet or a HFD (16 wk). Blood glucose concentration in mice fasted overnight or fed *ad libitum* was measured (mean \pm SEM; n = 35 ~ 50; *, $p < 0.05$; **, $p < 0.01$; ***, $p < 0.001$).

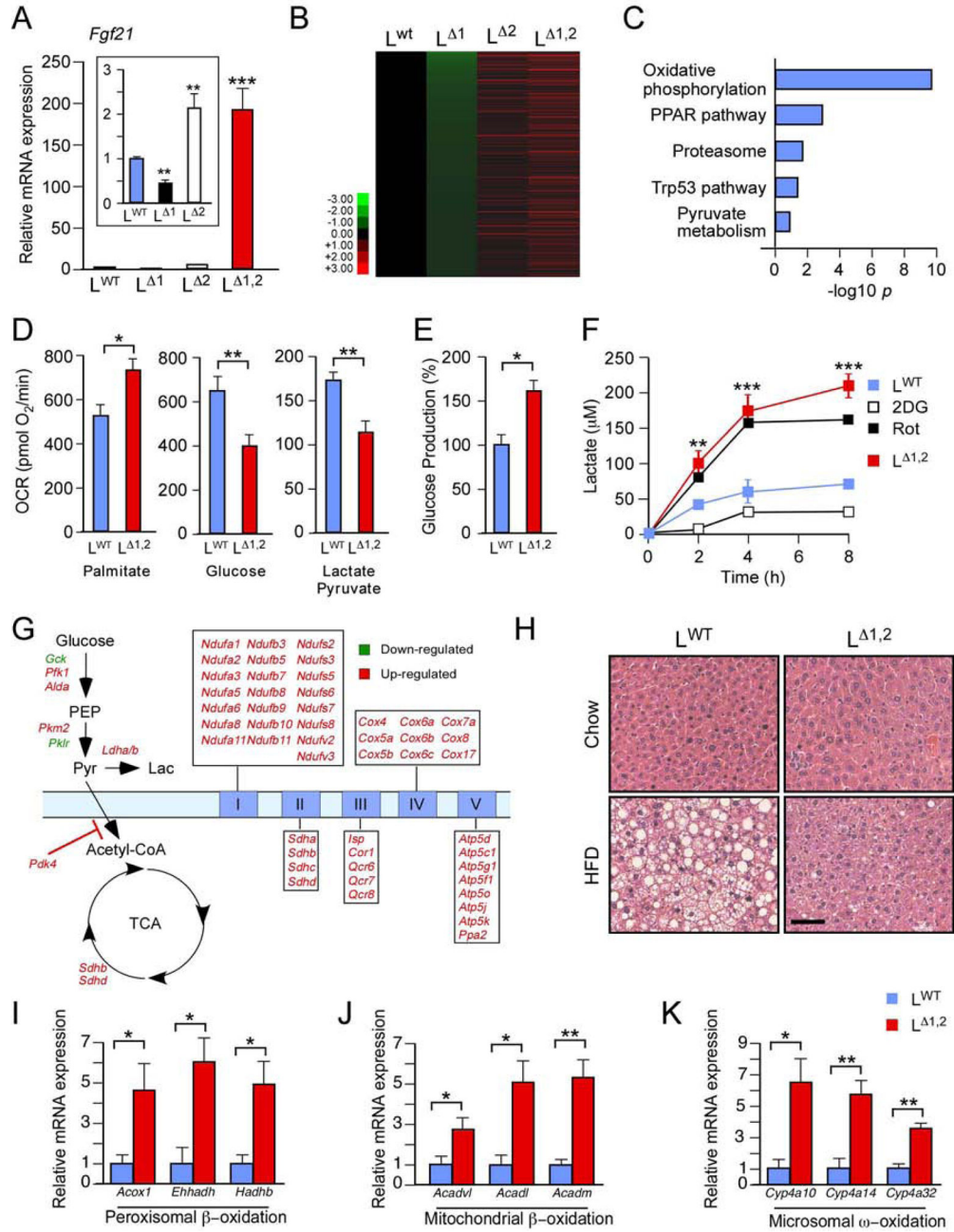


Figure 3. Hepatic JNK suppresses the PPAR α pathway and fatty acid oxidation
(A) *Fgf21* mRNA expression by primary hepatocytes obtained from L^{WT}, L¹, L² and L^{1,2} mice was measured by quantitative RT-PCR assays (mean \pm SEM; n = 6; **, p < 0.01; ***, p < 0.001).
(B, C) Heatmap representation of RNA-seq analysis of hepatic genes in overnight fasted HFD-fed mice with the expression profile L¹ < L^{WT} < L² < L^{1,2}. The genes are displayed with lowest expression (*top*) to highest expression (*bottom*) in L¹ liver. Gene ontology analysis of these genes is presented (C).

(D–F) Seahorse XF24 analysis was performed using primary hepatocytes isolated from L^{WT} and L^{1,2} mice. Mitochondrial oxygen consumption rate (OCR) in the presence of 200 μM palmitate/BSA, 15 mM glucose, or 1 mM pyruvate / 10 mM lactate (D). Glucose production rate per μg protein in the presence of 1 mM pyruvate / 10 mM lactate (E). Lactate production by L^{WT} and L^{1,2} mice hepatocytes (incubated with 15 mM glucose) and the effect of treatment of L^{WT} hepatocytes with 15 mM 2-deoxyglucose (2DG) or 100 nM rotenone (Rot). (F). The data presented are the mean ± SEM; n=10–15; *, $p < 0.05$; **, $p < 0.01$; ***, $p < 0.001$.

(G) Differentially expressed glycolysis, tricarboxylic acid cycle, and electron transport chain genes identified by RNA-seq analysis in the liver of HFD-fed L^{1,2} mice compared with HFD-fed L^{WT} are illustrated ($p_{adj} < 0.05$).

(H) L^{WT} and L^{1,2} mice were fed a chow diet or a HFD (16 weeks). Sections of the liver were stained with hematoxylin and eosin. Bar, 25 μm.

(I–K) Gene expression in the liver of overnight-fasted L^{WT} and L^{1,2} mice was measured by quantitative RT-PCR assays of mRNA (mean ± SEM; n = 8; **, $p < 0.01$; ***, $p < 0.001$). See also Figures S3 & S4.

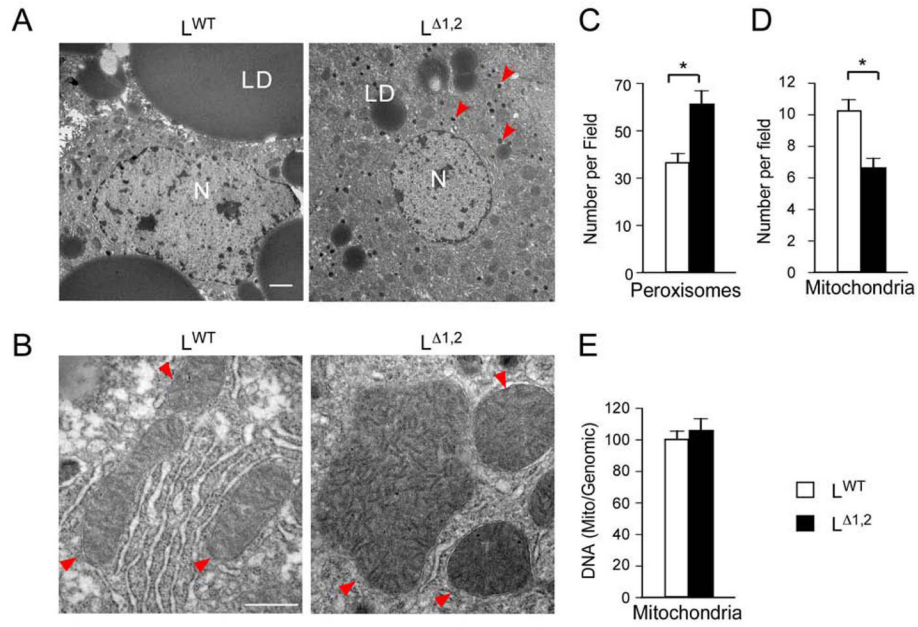


Figure 4. Hepatic JNK-deficiency increases peroxisome number and mitochondrial size (A, B) L^{WT} and L^{Δ1,2} mice were fed a HFD (16 wks). Sections of the liver were examined by transmission electron microscopy. Representative images are presented. Key: nucleus (N); lipid droplet (LD). Arrow heads indicate peroxisomes (A) and mitochondria (B). Bar, 2 μm (A) and 0.5 μm (B). (C, D) The number of peroxisomes (C) and mitochondria (D) per field was measured (mean ± SEM; n = 30; *, p < 0.05). (E) Relative mitochondrial DNA copy number was measured (mean ± SEM; n = 3).

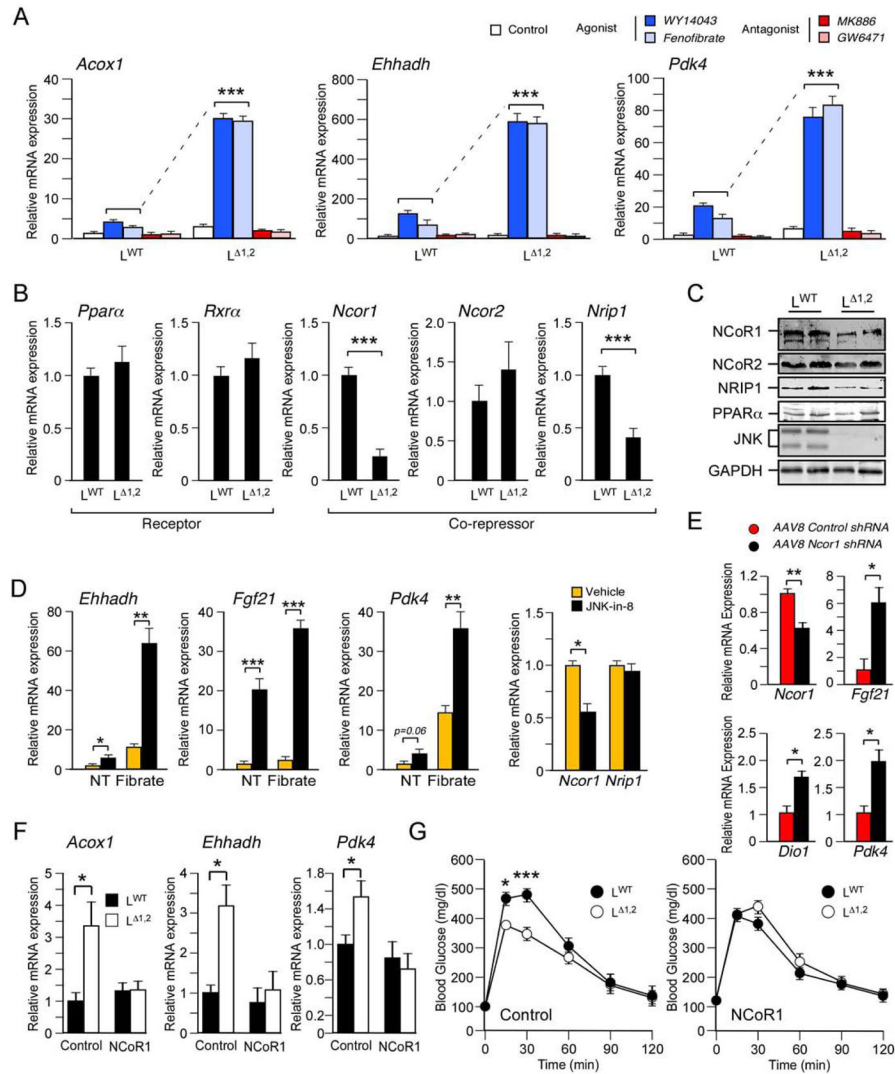


Figure 5. Hepatic JNK inhibits PPAR α -dependent gene expression

(A) Primary hepatocytes were obtained from L^{WT} and L ^{Δ 1.2} mice and incubated with solvent (DMSO, Control), PPAR α agonists (50 μ M WY14043 or 100 μ M Fenofibrate), or PPAR α antagonists (10 μ M GW6471 or 20 μ M MK886) for 16h. PPAR α target gene (*Acox1*, *Ehhadh*, and *Pdk4*) expression was examined by measurement of mRNA by quantitative RT-PCR analysis (mean \pm SEM; n = 6; ***, $p < 0.001$).

(B) The expression of *Ppara*, *Rxra*, *Ncor1*, *Ncor2*, and *Nrip1* mRNA by L^{WT} and L ^{Δ 1.2} primary hepatocytes was measured by quantitative RT-PCR analysis (mean \pm SEM; n = 6; ***, $p < 0.001$).

(C) L^{WT} and L ^{Δ 1.2} primary hepatocytes were examined by immunoblot analysis by probing with antibodies to PPAR α , NCoR1, NCoR2, NRIP1, JNK, and GAPDH.

(D) Primary wild-type hepatocytes were treated (12 h) with DMSO (vehicle) or 1 μ M JNK-in-8 (a small molecule JNK inhibitor) prior to measurement of mRNA expression by quantitative RT-PCR analysis (mean \pm SEM; n = 6; *, $p < 0.05$; **, $p < 0.01$; ***, $p < 0.001$).

0.001). The effect of treatment (8 h) of the hepatocytes with DMSO (NT) or 100 μ M Fenofibrate (Fibrate) was examined.

(E) Recombinant AAV8 vectors were employed to express *Control shRNA* or *Ncor1 shRNA* in the liver of HFD-fed (4 wks.) of L^{WT} and L^{1,2} mice. Hepatic mRNA expression at 10 ~ 16 days post-infection was examined by quantitative RT-PCR analysis (mean \pm SEM; n = 14 ~ 15; *, $p < 0.05$; **, $p < 0.01$).

(F, G) NCoR1 or GFP (Control) were expressed in the liver of HFD-fed (4 wks.) of L^{WT} and L^{1,2} mice using recombinant adenovirus vectors (10 ~ 16 days). The hepatic expression of *Acox1*, *Ehhadh* & *Pdk4* mRNA was measured by quantitative RT-PCR analysis (F). The mice were examined by glucose tolerance tests (G). The data presented are the mean \pm SEM (n = 6; *, $p < 0.05$; ***, $p < 0.001$).

See also Figures S5 & S6.

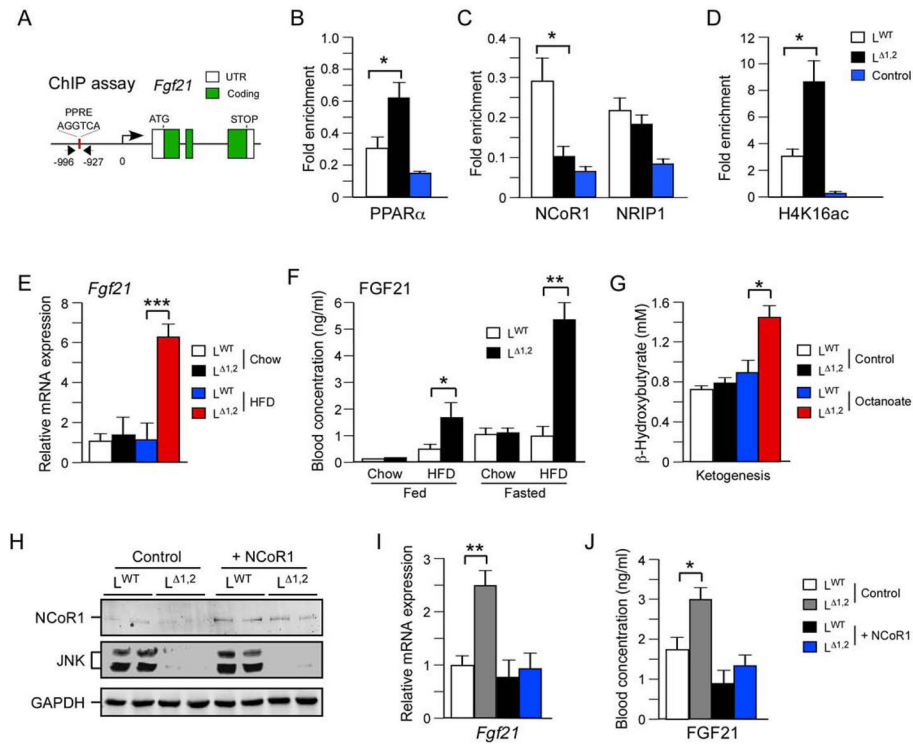


Figure 6. The FGF21 pathway is repressed by JNK

(A–D) Chromatin immunoprecipitation (ChIP) assays were performed using liver isolated from overnight fasted L^{WT} and $L^{1,2}$ mice with antibodies to non-immune immunoglobulin (Control), PPAR α , NCoR1, NRIP1, and acetyl-lysine¹⁶ histone H4 (H4K16ac). The fold enrichment of a fragment of the *Fgf21* promoter with a PPRE site was measured by quantitative PCR analysis (mean \pm SEM; $n = 6$; $p < 0.05$).

(E) The hepatic expression of *Fgf21* mRNA in overnight fasted mice was examined by quantitative RT-PCR analysis (mean \pm SEM; $n = 8$; ***, $p < 0.001$).

(F) The concentration of FGF21 in the blood of chow-fed and HFD-fed L^{WT} and $L^{1,2}$ mice was measured by ELISA. Blood was collected from mice fed *ad libitum* or fasted overnight (mean \pm SEM; $n=6$; *, $p < 0.05$; **, $p < 0.01$).

(G) Ketone body production was measured in overnight-fasted L^{WT} and $L^{1,2}$ mice challenged (6 h) without (Control) and with Octanoate (mean \pm SEM; $n = 5$; *, $p < 0.05$).

(H–J) NCoR1 or GFP (Control) were expressed in the liver of HFD-fed (4 wks.) L^{WT} and $L^{1,2}$ mice using recombinant adenovirus vectors (10 ~ 16 days). The mice were fasted overnight and hepatic expression of NCoR1 and GAPDH were examined by immunoblot analysis (H). The amount of *Fgf21* mRNA was measured by quantitative RT-PCR analysis (I) and the concentration of FGF21 in the blood was measured by ELISA (J). The data presented are the mean \pm SEM; $n = 6$; *, $p < 0.05$; **, $p < 0.01$.

See also Figure S7.

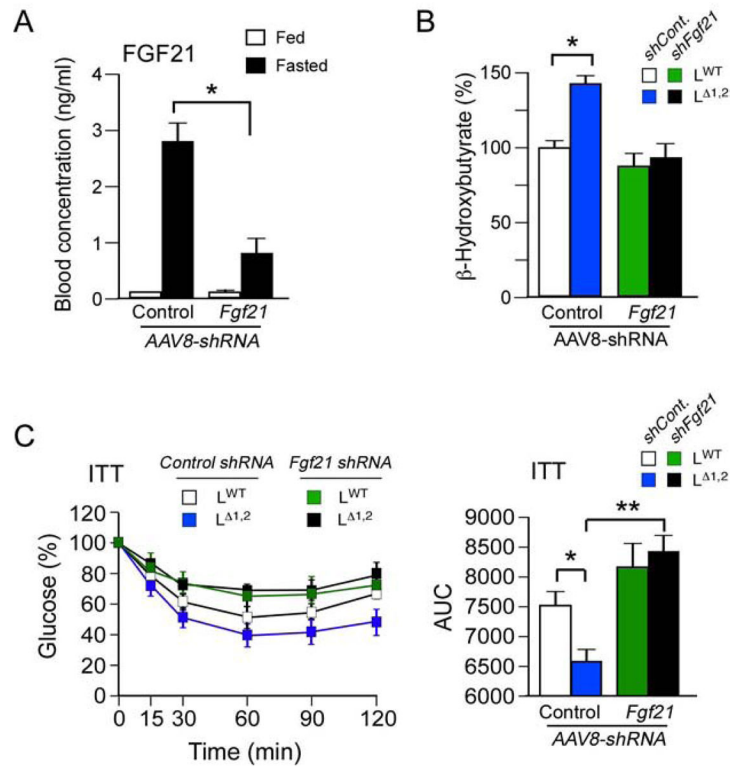


Figure 7. FGF21 mediates metabolic effects of hepatic JNK-deficiency

(A) AAV8 vectors were employed to express *Control shRNA* and *Fgf21 shRNA* in the liver. The mice were fed a HFD (4 wk). FGF21 in the blood of mice fed ad-libitum or fasted overnight was measured by ELISA (mean \pm SEM; n = 6; *, $p < 0.05$).

(B) Ketogenesis was examined in HFD-fed mice that were fasted overnight and then challenged with octanoate (6 h) by measurement of blood β -hydroxybutyrate (mean \pm SEM; n = 15 ~ 30; $p < 0.05$). The data are normalized to blood β -hydroxybutyrate in control mice at 0 h (100%).

(C) Insulin tolerance tests (ITT) were performed on HFD-fed mice. The time course of blood glucose clearance and the area under the curve (AUC) are presented (mean \pm SEM; n = 15 ~ 30; *, $p < 0.05$; **, $p < 0.01$).